Direct evidence of spin filtering across MnFe_2O_4 tunnel barrier by Meservey-Tedrow experiment

S. Matzen, J.-B. Moussy, G. X. Miao, J. S. Moodera

Direct evidence of spin filtering across MnFe$_2$O$_4$ tunnel barrier by Meservey-Tedrow experiment

S. Matzen,[1] J.-B. Moussy,[1] G. X. Miao,[2] and J. S. Moodera[2,3]

[1]*CEA-Saclay, IRAMIS, SPCSI, 91191 Gif-Sur-Yvette, France*

[2]*Francis Bitter Magnet Laboratory, Massachusetts Institute of Technology, Cambridge, Massachusetts 02139, USA*

[3]*Physics Department, Massachusetts Institute of Technology, Cambridge, Massachusetts 02139, USA*

A spin filtering effect has been evidenced in epitaxial MnFe$_2$O$_4$ tunnel barriers directly by Meservey-Tedrow experiments. The asymmetry of the Zeeman-split tunneling conductance curves of the superconducting Al spin analyzer in Pt(111)/MnFe$_2$O$_4$(111)/γ-Al$_2$O$_3$(111)/Al tunnel junctions revealed a positive spin-polarization (up to $+9\%$), proving the potential of manganese ferrite for generation of a spin-polarized current. A negatively polarized spin filtering being expected theoretically, different mechanisms are discussed to explain both sign and amplitude of the measured spin-polarization.

PACS number(s): 75.47.Lx, 72.25.−b, 85.75.−d

I. INTRODUCTION

The efficient injection of spin-polarized electron currents into a semiconductor is one of the main goals in the field of spintronics. The generation of highly spin-polarized electrons is mostly based on the electronic transport through a ferromagnetic metal or semiconductor, acting as the source of polarized carriers. The tunneling of spin-polarized electrons from a ferromagnetic material, through an insulating tunnel barrier, into a semiconductor is one of the most promising ways to achieve efficient spin injection,[1] that otherwise is usually limited by the conductivity mismatch between the ferromagnet and semiconductor.[2] In the last few years, another interesting approach, known as spin filtering,[3] has been investigated to create highly spin-polarized electrons. In this approach, a ferromagnetic tunnel barrier is used as a source of polarized electrons. More precisely, the spin filter effect originates from the exchange splitting of the conduction band energy levels (ΔE_{ex}) of the magnetic insulator. Consequently, the tunnel barrier heights for spin-up (ϕ_{up}) and spin-down (ϕ_{down}) electrons are not the same, leading to a higher probability of tunneling for one of the two spin orientations. The spin filtering efficiency is defined by the spin-polarization (P_{SF}) of the current tunneling through the magnetic tunnel barrier: $P_{SF} = (J_{up} - J_{down})/(J_{up} + J_{down})$, $J_{up,down}$ being the spin-up (spin-down) tunnel currents. Here, $J_{up,down}$ is exponentially dependent upon the corresponding barrier height: $J_{up,down} \sim \exp(-\phi_{up,down}^{1/2})$. In addition, other factors may play a significant role in the preferential transmission of electrons through the tunnel barrier, as described by the work of Mazin[4] and Tsymbal *et al.*,[5,6] revealing the complexity of the spin-dependent tunneling mechanism. Spin filters are promising for the future generation of spin-based devices because they could generate 100% spin-polarized electron currents[7] and be combined with any nonmagnetic semiconductor.

The spin filtering effect has been first demonstrated at low temperatures in EuS magnetic tunnel barriers,[8] and then in oxide barriers [EuO (Ref. 9) and BiMnO$_3$ (Ref. 10)]. However, the low Curie temperature (T_c) of these materials limits their spin filtering capability to temperatures well below room temperature. More recently, the spinel ferrites have gained much attention due to their potential as spin filters at room temperature. This class of materials includes ferrimagnetic and insulating compounds with high T_c values, such as NiFe$_2$O$_4$ ($T_c = 850$ K), CoFe$_2$O$_4$ ($T_c = 793$ K), and MnFe$_2$O$_4$ ($T_c = 573$ K). The spin filtering capability of NiFe$_2$O$_4$ (Ref. 11) and CoFe$_2$O$_4$ (Refs. 12–17) tunnel barriers has been reported only recently, due to the difficulty of fabricating high-quality epitaxial ultrathin films of these complex oxides.[18] Up to now, ferrites tunnel barriers have shown spin filtering efficiencies of $P_{SF} = 22\%$ for NiFe$_2$O$_4$ at 4 K[11] and $P_{SF} = -44\% (-4\%)$ for CoFe$_2$O$_4$ at 10 K (290 K).[13,15] A maximum spin-polarization of -8% has been obtained at room temperature in CoFe$_2$O$_4$-based nanojunctions.[17]

MnFe$_2$O$_4$ is another promising candidate as a room temperature spin filter. As its predicted ΔE_{ex} in the normal spinel structure (3.85 eV)[19] is higher than for the NiFe$_2$O$_4$ (1.21 eV) and CoFe$_2$O$_4$ (1.28 eV) inverse spinel oxides, MnFe$_2$O$_4$ could lead to better spin filtering efficiencies. Recently, we have grown high-quality epitaxial ultrathin films of MnFe$_2$O$_4$ with good magnetic and insulating properties, proving the high potential of MnFe$_2$O$_4$ to be used as a magnetic tunnel barrier at room temperature.[20] The polarization of the tunnel current can be extracted from tunnel magnetoresistance (TMR) measurements, using another ferromagnetic layer (FM) as spin analyzer.[10] This technique requires a magnetic decoupling between the spin filter and the spin analyzer. This is obtained most of the time by the insertion of a nonmagnetic layer (NM). In addition, it is necessary to know the spin-polarization of the FM/NM layers to extract the spin filtering efficiency. A direct determination of P_{SF} can be performed by the Meservey-Tedrow technique, using a superconducting aluminum electrode as the spin detector.[21] In this paper, we use the Meservey-Tedrow technique to study the spin filtering capabilities of MnFe$_2$O$_4$ magnetic tunnel barriers.

II. EXPERIMENT

MnFe$_2$O$_4$(111) thin films with thicknesses down to 2 nm have been grown by oxygen-assisted molecular beam epitaxy (MBE) on Pt(111) buffered α-Al$_2$O$_3$(0001) substrates. The films have been deposited at 450 °C from Knudsen effusion cells of Mn, Fe with an oxygen partial pressure $P(O_2)$ in the plasma source in the 0.2–0.34 Torr range (corresponding to a pressure range of $2 \times 10^{-8} - 1 \times 10^{-7}$ Torr inside the evaporation chamber). The ultrathin films exhibit high

structural order, with insulating and ferrimagnetic behavior at room temperature as described in Ref. 20. For the spin filtering measurements, epitaxial $MnFe_2O_4(111)/\gamma$-$Al_2O_3(111)$ double barriers have been grown following a procedure inspired by the growth of $CoFe_2O_4(111)/\gamma$-$Al_2O_3(111)$ tunnel barriers.[14]

The growth parameters have been adjusted to obtain the spinel structure for both $MnFe_2O_4$ and γ-Al_2O_3 layers with a two-dimensional growth mode and correct stoichiometries. Special attention has been paid so that the deposition of the γ-Al_2O_3 layer does not affect the oxidation state of $MnFe_2O_4$. All double barriers grown under $P(O_2)$ between 0.2 and 0.34 Torr exhibited similar x-ray photoemission spectroscopy (XPS) and Auger electron spectroscopy spectra (not shown). Consequently, no noticeable change in the oxidation state of the films has been observed with the variation of $P(O_2)$ during growth. Finally, the ferrite ultrathin films clearly show a ferrimagnetic behavior,[20] with a net magnetization of 350 kA/m at 2 T and a coercivity around 430 Oe for a 2-nm-thick film at 10 K (the deposition of the γ-Al_2O_3 layer does not affect the magnetic properties). The spin-polarized transport measurements have been performed at high field (3.3 T) on $MnFe_2O_4$ barriers that were then close to the magnetic saturation.

To study the spin filtering capability of the $MnFe_2O_4$ barriers, a superconducting Al electrode is deposited on the $MnFe_2O_4/\gamma$-Al_2O_3 bilayers to act as a spin analyzer by the Meservey-Tedrow technique. This last step in the samples' processing is realized in a separate thermal evaporation chamber. First, the surface of the γ-Al_2O_3 layer is treated by gentle oxygen plasma in order to clean it from any contamination due to the exposure to air and thus ensure a good quality of the interface with Al. Then, an amorphous alumina layer (8 nm thick) is deposited through a shadow mask by electron-beam evaporation to cover the edges thus defining a long strip of $MnFe_2O_4/\gamma$-Al_2O_3 (500 μm wide). Finally, the sample is cooled down to 77 K and a 4.2-nm-thick Al layer is deposited as cross strips, which allows defining $Pt/MnFe_2O_4/\gamma$-Al_2O_3/Al tunnel junctions with areas of $\sim$500 $\times$ 200 μm^2.

III. RESULTS AND DISCUSSION

The tunnel junctions have been cooled down to 0.45 K in a ^{3}He cryostat to perform the spin-polarized transport measurements well below the superconducting transition temperature of Al. The superconducting transition temperature of the 4.2-nm Al was 2.3 K. Tunneling dynamic conductance (dI/dV) versus bias voltage curves have been measured with a magnetic field up to 3.3 T applied in the films plane. The data for a $Pt/MnFe_2O_4(4$ nm$)/\gamma$-$Al_2O_3(1.1$ nm$)/Al(4.2$ nm$)$ junction $[P(O_2) = 0.34$ Torr$]$ are shown in Fig. 1(a). The dI/dV curves at zero magnetic field for all junctions present symmetric peaks defining the superconducting energy gap of 0.87 meV of Al. These sharp symmetric peaks and the negligible conductance at zero bias confirm the high quality of the tunnel junctions. The application of a magnetic field produces a Zeeman splitting of the Al quasiparticle density of states. The measured Zeeman split dI/dV curves are clearly asymmetric, proving that the tunneling current is spin-polarized. A spin-polarization of 6% ($\pm$1%) is extracted from the relative conductance peaks' heights at 3.3 T by taking
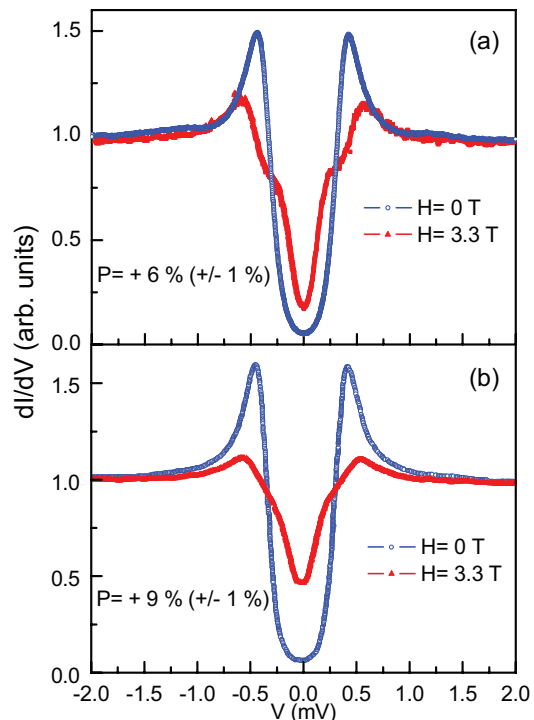

FIG. 1. (Color online) Tunneling dynamic conductance (dI/dV) versus bias voltage curves measured at 0.45 K under zero magnetic field and 3.3 T for (a) a $Pt/MnFe_2O_4(4$ nm$)/\gamma$-$Al_2O_3(1.1$ nm$)/Al(4.2$ nm$)$ junction $[P(O_2) = 0.34$ Torr$]$ and (b) a $Pt/MnFe_2O_4(3.5$ nm$)/\gamma$-$Al_2O_3(0.6$ nm$)/Al(4.2$ nm$)$ junction $[P(O_2) = 0.2$ Torr$]$.

into account the estimation of the peaks' positions.[21] As there is no ferromagnetic electrode in the $Pt/MnFe_2O_4/\gamma$-Al_2O_3/Al tunnel junctions, the spin-polarization can only be explained by spin filtering in the $MnFe_2O_4$ barrier. This result is very encouraging since it marks the first successful revelation of spin filtering in a manganese ferrite tunnel barrier.

Following this direct demonstration of the spin filtering capability of $MnFe_2O_4$ tunnel barriers, two main observations can be made about the sign and amplitude of the spin-polarization. First, the positive sign seems in contradiction with the expected negative polarization for $MnFe_2O_4$ from band structures calculations.[19] As the Meservey-Tedrow technique is undoubtedly the most direct measurement of the polarization of a tunneling current, this result shows that there is some additional factor, other than the density of states (DOS) in the $MnFe_2O_4$ conduction band, influencing the overall spin-polarized tunneling process. Tsymbal and Pettifor,[5] based on theory, have pointed out that the spin-polarization of the tunneling current depends strongly on the type of covalent bonding at the interface between the ferromagnet and the insulator in magnetic tunnel junctions. Other Meservey-Tedrow experiments have already revealed unexpected polarizations, in contradiction with TMR measurements, in particular in $Co/SrTiO_3/Al$ (Refs. 22 and 23) and $Pt/CoFe_2O_4/Al_2O_3/Al$ (Refs. 14 and 13) tunnel junctions. For both systems, the authors proposed that the wave-function symmetry of the Al detector may actually determine the sign of polarization.[14,22] In our tunnel junctions, the alignment

between the bands in the epitaxial ferrite barrier with the bands of the Al spin detector could result in the preferential detection of the highly delocalized sp electrons, explaining the measured positive P_{SF}. Additional factors may also play a significant role in the preferential transmission of electrons through the tunnel barrier. Lüders *et al.* proposed a complex model to explain the positive P_{SF} measured by TMR in NiFe$_2$O$_3$/SrTiO$_3$/La$_{2/3}$Sr$_{1/3}$MnO$_3$ spin filters,[24] based on the difference in decay rates for spin-up and spin-down electrons. In our Meservey-Tedrow experiments performed at very low bias (<2 mV), the transport is governed by direct tunneling mechanism, and thus the spin-dependent tunnel current densities ($J_{up,down}$) are likely modified by the corresponding tunnel matrix elements[4] in addition to electrons mobilities. It may thus be necessary to consider, in addition to spin-dependent barrier heights, global transmission coefficients for electrons through the barrier defined by tunnel matrix elements in order to understand the sign of P_{SF}. Obviously, complex energy band structure calculations for the whole MnFe$_2$O$_4$/Al$_2$O$_3$/Al system are required to give better predictions on the spin-polarization.

It may be noted that the amplitude of the measured spin-polarization remains quite low in comparison with what could be expected from a MnFe$_2$O$_4$ spin filter, probably due to defect states in the barrier, creating parallel spin-independent conduction channels.[15,25,26] Ramos *et al.* have shown the predominant effect of oxygen vacancies on spin filtering of CoFe$_2$O$_4$:[14] by increasing the oxygen pressure during the growth of the ferrite barrier, P_{SF} has been increased from 6% to 26%. Figure 2 shows the temperature dependence of our junctions resistance-area product ($R_J A$) for various $P(O_2)$ during growth. The observed exponential increase at low temperatures indicates a thermally activated conduction mechanism, suggesting the presence of defects in the barriers. The temperature dependence of the resistance was significantly lower for the high $P(O_2)$ grown barriers, as observed in conductive atomic force microscopy measurements at 300 and 10 K, showing little difference of resistance in highly oxidized MnFe$_2$O$_4$ ultrathin films (not shown). This shows that oxygen vacancies influence the tunneling properties, creating defect states in the band gap that act in lowering the effective barrier height for the tunneling electrons, and thus introducing a stronger temperature dependence of the resistance. It is interesting to note that the changes of oxidation state in our MnFe$_2$O$_4$ barriers have only been evidenced in the tunneling experiments due to their high sensitivity to the presence of minor defects. All standard chemical and magnetic characterization techniques could not detect the presence of oxygen vacancies for $P(O_2) \geqslant 0.2$ Torr. The $I(V)$ curves measured at low temperature look similar to typical $I(V)$ curves for Al$_2$O$_3$ tunnel barriers, showing a well-established tunneling transport consistent with the data presented in Fig. 1. No further quantitative study has been performed due to the presence of defects that would not give reliable parameters for the effective MnFe$_2$O$_4$/Al$_2$O$_3$ double barriers.

While changing $P(O_2)$ between 0.2 and 0.34 Torr is shown to significantly affect the oxygen vacancies concentration, no visible modification of the spin filtering efficiency is measured [Fig. 1(b)]. A spin-polarization of 9% (± 1%) has been achieved by spin filtering through the MnFe$_2$O$_4$ tunnel
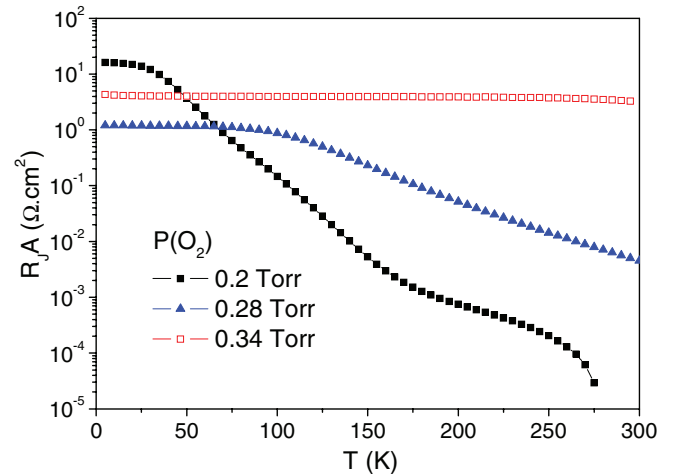

FIG. 2. (Color online) Temperature dependence of three junctions resistance-area products ($R_J A$), where MnFe$_2$O$_4$ was grown with different oxygen pressure $P(O_2)$.

barrier prepared with a $P(O_2)$ of 0.2 Torr that showed the strong $R_J A(T)$ dependence, as seen in Fig. 2. These results suggest that there are other types of defects than oxygen vacancies in the barriers that do not affect visibly $R_J A(T)$ but limit the spin-polarization, such as cationic disorder and antiphase boundaries. These two types of defects certainly can be expected to modify the electronic structure of MnFe$_2$O$_4$ and thus explaining the limited spin filtering seen here. A cationic disorder could, for example, be created by a small deviation from stoichiometry (that remains undetectable by XPS analysis) or by a small deviation in the cationic distribution among octahedral and tetrahedral sites of the spinel structure.[20] Furthermore, antiphase boundaries are well-known structural defects in ferrite thin films that affect their magnetic properties by inducing additional antiferromagnetic couplings. The reduced magnetization in thin films could then decrease the conduction band exchange splitting and limit the spin filtering efficiency. In addition, these stacking faults in the cationic sublattice could act as preferential conduction channels without any spin filtering effect, reducing the spin-polarization of the current through the MnFe$_2$O$_4$ barrier. Very recently, we have shown that the spin-polarization in CoFe$_2$O$_4$ spin filters can be increased by limiting the contribution of defects if the junctions' size is reduced to the nanoscale.[17] The search for more suitable substrates (such as spinel MgAl$_2$O$_4$) also offers promising perspectives to get higher spin-polarization, by promoting the growth of ultrathin ferrite films without antiphase boundaries.[27]

IV. CONCLUSION

To conclude, the spin filtering capability of manganese ferrite tunnel barriers has been directly demonstrated by the Meservey-Tedrow technique. A spin-polarization up to 9% has been achieved for the tunneling current by spin filtering through MnFe$_2$O$_4$. The positive sign of the spin-polarization values has revealed that spin-dependent tunneling with ferrite barriers is a complex mechanism that cannot be described by a simple model based only on the barrier heights for the two spin

orientations. To give better predictions on the spin filtering, energy band structure calculations should especially consider decay rates of spin-up and spin-down electrons through the barrier and include the effect of the spin analyzer. Moreover, our results suggest that the spin-polarization could be further limited by the presence of defects, other than oxygen vacancies in the ferrite barriers. In this context, the control of the growth of ferrite ultrathin films without antiphase boundaries appears particularly crucial in order to get higher spin-polarization.

[1] A. Fert and H. Jaffrès, Phys. Rev. B **64**, 184420 (2001).

[2] E. I. Rashba, Phys. Rev. B **62**, R16267 (2000).

[3] J. S. Moodera, T. S. Santos, and T. Nagahama, J. Phys.: Condens. Matter **19**, 165202 (2007).

[4] I. I. Mazin, Phys. Rev. Lett. **83**, 1427 (1999).

[5] E. Y. Tsymbal and D. G. Pettifor, J. Phys.: Condens. Matter **9**, L411 (1997).

[6] E. Y. Tsymbal, K. D. Belashchenko, J. P. Velev, S. S. Jaswal, M. van Schilfgaarde, I. I. Oleynik, and D. A. Stewart, Prog. Mater. Sci. **52**, 401 (2007).

[7] J. S. Moodera, R. Meservey, and X. Hao, Phys. Rev. Lett. **70**, 853 (1993).

[8] J. S. Moodera, X. Hao, G. A. Gibson, and R. Meservey, Phys. Rev. Lett. **61**, 637 (1988).

[9] T. S. Santos and J. S. Moodera, Phys. Rev. B **69**, 241203 (2004).

[10] M. Gajek, M. Bibes, A. Barthélémy, K. Bouzehouane, S. Fusil, M. Varela, J. Fontcuberta, and A. Fert, Phys. Rev. B **72**, 020406 (2005).

[11] U. Lüders, M. Bibes, K. Bouzehouane, E. Jacquet, J.-P. Contour, S. Fusil, J. Fontcuberta, A. Barthélémy, and A. Fert, Appl. Phys. Lett. **88**, 082505 (2006).

[12] M. G. Chapline and S. X. Wang, Phys. Rev. B **74**, 014418 (2006).

[13] A. V. Ramos, M.-J. Guittet, J.-B. Moussy, R. Mattana, C. Deranlot, F. Petroff, and C. Gatel, Appl. Phys. Lett. **91**, 122107 (2007).

[14] A. V. Ramos, T. S. Santos, G. X. Miao, M.-J. Guittet, J.-B. Moussy, and J. S. Moodera, Phys. Rev. B. **78**, 180402(R) (2008).

[15] Y. K. Takahashi, S. Kasai, T. Furubayashi, S. Mitani, K. Inomata, and K. Hono, Appl. Phys. Lett. **96**, 072512 (2010).

[16] F. Rigato, S. Piano, M. Foerster, F. Giubileo, A. M. Cucolo, and J. Fontcuberta, Phys. Rev. B **81**, 174415 (2010).

[17] S. Matzen, J.-B. Moussy, R. Mattana, K. Bouzehouane, C. Deranlot, and F. Petroff, Appl. Phys. Lett. **101**, 042409 (2012).

[18] Y. Suzuki, Annu. Rev. Mater. Res. **31**, 265 (2001).

[19] Z. Szotek, W. M. Temmerman, D. Kodderitzsch, A. Svane, L. Petit, and H. Winter, Phys. Rev. B **74**, 174431 (2006).

[20] S. Matzen, J.-B. Moussy, R. Mattana, K. Bouzehouane, C. Deranlot, F. Petroff, J. C. Cezar, M.-A. Arrio, Ph. Sainctavit, C. Gatel, B. Warot-Fonrose, and Y. Zheng, Phys. Rev. B **83**, 184402 (2011).

[21] R. Meservey and P. M. Tedrow, Phys. Rep. **238**, 173 (1994).

[22] A. Thomas, J. S. Moodera, and B. Satpati, J. Appl. Phys. **97**, 10C908 (2005).

[23] J. M. De Teresa, A. Barthélémy, A. Fert, J.-P. Contour, F. Montaigne, and P. Seneor, Science **286**, 507 (1999).

[24] U. Lüders, M. Bibes, S. Fusil, K. Bouzehouane, E. Jacquet, C. B. Sommers, J. P. Contour, J. F. Bobo, A. Barthélémy, A. Fert, and P. M. Levy, Phys. Rev. B **76**, 134412 (2007).

[25] M. Foerster, D. F. Gutierrez, F. Rigato, J. M. Rebled, F. Peiro, and J. Fontcuberta, Appl. Phys. Lett. **97**, 242508 (2010).

[26] M. Foerster, D. F. Gutierrez, J. M. Rebled, E. Arbelo, F. Rigato, M. Jourdan, F. Peiro, and J. Fontcuberta, J. Appl. Phys. **111**, 013904 (2012).

[27] S. Matzen, J.-B. Moussy, R. Mattana, F. Petroff, C. Gatel, B. Warot-Fonrose, J. C. Cezar, A. Barbier, M.-A. Arrio, and Ph. Sainctavit, Appl. Phys. Lett. **99**, 052514 (2011).